Proceedings of the Second International Conference on Press-in Engineering 2021, Kochi, Japan – Matsumoto et al (eds)

Reliability analysis on cantilever retaining walls embedded into stiff ground (Part 1: Contribution of major uncertainties in the elasto-plastic subgrade reaction method)

N. Suzuki
GIKEN LTD., Tokyo, Japan

K. Nagai
The University of Tokyo, Tokyo, Japan

T. Sanagawa
Railway Technical Research Institute, Tokyo, Japan

ABSTRACT: Reliability analysis was performed for cantilever retaining walls embedded in two-layer ground with deep stiff ground. The analysis was conducted by treating soil/rock properties, uniform surcharge, depth of the rock layer surface and yield strength of steel as random variables based on various previous works. We calculated sensitivity factors of each variable for the limit states in the persistent design situation. The contributions of scatters of the depth of the rock layer surface are high in the order of rotational failure, deformation failure, and flexural failure. The results suggest that the scatter of the depth of the rock layer surface should be considered, especially if varied horizontal layer is expected and the deformation failure or the rotational failure are determinants of the design.

1 INTRODUCTION

1.1 *Overview*

More and more embedded cantilever retaining walls have been applied when retrofitting structures and widening roads in Japan to minimize the impact on daily traffic (Miyanohara et al. 2018 and Suzuki & Kimura 2021). Since the walls became higher and more rigid, the required embedment depth became longer in adapting the semi-infinite embedment condition. That resulted in a longer construction period and a more expensive construction, especially in stiff ground.

Thus, TC1 of International Press-in Association (IPA) has tried to rationalize the design of cantilever steel pipe pile retaining walls in the stiff ground. The authors believe that two issues are important for applying short embedment; the varied horizontal layer (Figure 1) and the strict limits on the displacement of the wall top.

Fine boundaries of strata require high quality investigation and sampling for hard/medium rock (EN 1997-2. 2007). However, detailed geotechnical investigations are rarely conducted for retaining walls with long horizontal extensions, while a varied horizontal layer has been taking on renewed importance by pile foundations (e.g. Zhang & Dasaka 2010 and JGCA 2017).

The failure modes of cantilever retaining walls are flexural and rotational failure in the overall stability as well as piping and heaving. However, since cantilever steel pipe pile retaining road walls are usually constructed close to existing buildings (Suzuki & Kimura 2021), the displacement of the wall top has to be strict, and the wall deformation can be the determining factor of the wall specifications.

1.2 *Previous studies*

Many studies on the cantilever retaining walls have been conducted. For example, the observational data have been collected (Moormann 2004 and Michael 2001) and an easy method for reliability analysis has been introduced (Bak 2017).

Honjo & Otake (2014) compared the design values based on JRA (1999) with the field data for temporary earth retaining walls (including prop and anchor types walls) in Japan. They reported the statistics of model errors (including transformation

DOI: 10.1201/9781003215226-28

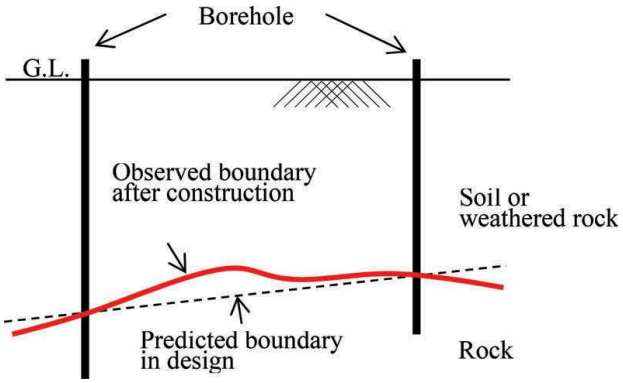

Figure 1. Illustrative example of varied horizontal layer.

errors) on the displacement (mean=0.70 and Coefficient of Variation [COV]=0.42) and on the bending moment (mean =0.69 and COV=0.62). The model errors in the design method were also reported by Zhang D. M. et al. 2015. They compared FEM and the Mobilized Strength Design (MSD) proposed by Osman & Bolton (2004), as well as 45 field data, and reported the model error of the displacement (FEM: mean=1.01 and COV=0.21).

Sivakumar & Basha (2008) performed sensitivity analysis with the cantilever steel sheet pile retaining walls against rotation about the base point and flexural failure using the Inverse First-Order Reliability Method (IFORM). They reported that the rotational failure is strongly influenced by the angle of shearing resistance and the yield strength for the flexural failure. In Japan, Shiozaki et al. (2010) conducted a reliability analysis of steel pipe pile walls for flexural failures and drew similar conclusions.

However, few studies consider the deformation failure, and no previous studies consider two-layer ground with the deep stiff ground. It is necessary to grasp the effect of embedment depth on the wall deformation to achieve a rational design by short embedment.

1.3 *Objective*

This study aims to grasp the effect of the depth of stiff ground on the failure of the cantilever retaining walls embedded in the two-layer ground. The results will provide useful information on which parameters are dominant in the reliability and when the reliability can be improved (i.e. in geotechnical investigation, design, or construction).

Section 2 introduces the methods of reliability analysis and random variables. Section 3 reports the contribution of random variables on each failure: deformation, flexural, and rotational failure.

2 METHODS

2.1 *Overview*

A calculation model was based on the one which has been commonly used in Japan. Analysis cases were decided with reference to the Japanese case histories of the rotary cutting press-in wall (Suzuki & Kimura 2021). The uncertainties of each random variable were obtained from various previous works, and then the sensitivity factors and the contribution factors of the variables were calculated.

2.2 *Models and analysis methods*

A cross-sectional view of the calculation model is shown in Figure 2a. The model assumed a cantilever retaining wall with 5 m excavation and two layers of soft soil and sandstone. The wall consisted of continuously pressed-in steel pipe piles with a distance of 180 mm between the pile surfaces. Because the drainage treatment was carried out between the steel piles, water pressure balanced between the excavation side and the backside. The average of the uniform surcharge was 10 kN/m^2 on the backside.

The deformation of the wall was calculated by the elasto-plastic subgrade reaction method, and the rotational stability and the critical embedment depth were confirmed by the limit equilibrium (Figure 2b). The subgrade reaction method is one of the simplest soil-structure interaction analyses, which models the wall as a beam and the ground as a series of horizontal springs (e.g. Gaba et al. 2017). Rotational resistance due to ground reaction at the pile tip was not taken into account since it was not observed in the FEM analysis for open-ended piles (Ishihama et al. 2019).

The allowable lateral displacement at the wall top was set as 50 mm, which is often used in the persistent design situation for road retaining walls in Tokyo, Japan. The lateral displacement was the alternative to the settlement of backside since the analysis of beam-columns on the elastic foundation could not estimate the settlement directly.

2.3 *Analysis case*

We analyzed 27 cases, including three cases of the depth of the rock layer surface, N-value of the rock layer, and the stiffness factor (Table 1).

The mean depths of the rock layer surface were 1.0, 3.0, and 5.0 m. About 3.0 m was the dominant depth for pile deformation ($1/\beta_0$).

The surface soil had an N-value of 10, and the sandstone had three converted N-values of 50, 300, and 1500 (Table 2). The stiffness, E_0, and strength parameters, c and ϕ, were estimated from SPT N-value by the equations in Appendix. This was

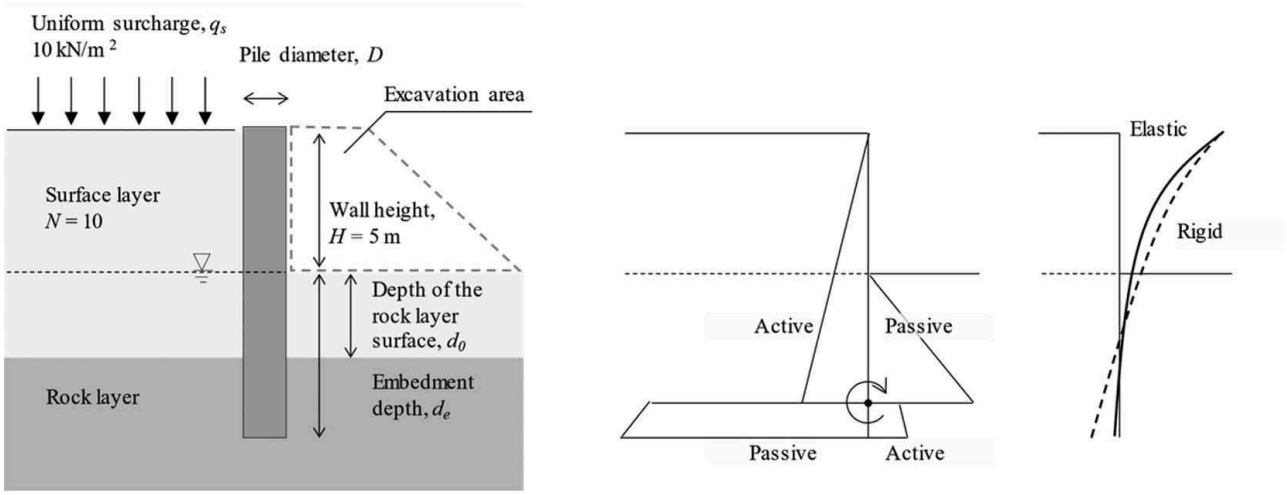

(a) Cross-sectional view of the calculation model (b) Idealized ultimate stress distribution (c) Deformation

Figure 2. Illustrative analysis model of cantilever retaining wall.

Table 1. Analysis case.

	Symbol	Unit	Values
Depth of the rock layer surface	d_0	m	1.0, 3.0, 5.0
N-value of the rock layer	N_r	-	50, 300, 1500
Factor of the stiffness of the wall	$\Sigma\beta_i d_i$	-	1.5, 2.0, 3.0

Table 2. Typical parameter of ground.

		Soil	Sandstone (Rock)		
N		10	50	300	1500
E_0	kN/m^2	2.8E+04	1.6E+05	5.5E+05	1.7E+06
ϕ	degree	32	38	42	46
c	kN/m^2	-	55	98	166
γ	kN/m^3	18.0	18.2	21.2	23.9

because it is sometimes difficult to sample rock masses that are heavily weathered or cracked, or due to existing buildings. And since the transformation equations in the range of N-values over 300 does not exist, this paper expanded the N value range of the equations shown in NEXCO RI (2016) to 1500. The typical values of the ground are shown in Table 2.

Stiffness factor, $\Sigma\beta_i d_i$, was 1.5, 2.0, and 3.0, which means rigid short piles, intermediate piles, and elastic long piles respectively (e.g. JRA 1999 used and Michael & John 2007 introduced the inverse of β_i);

$$\beta_i = \sqrt[4]{\frac{k_H B}{4EI}} \quad (1)$$

where B: Unit wall width, k_H: coefficient of lateral subgrade reaction, and EI: wall stiffness. As the embedment depth decreases, the behavior changes from the elastic to the rigid (Figure 2c), and the rotational failure becomes dominant.

Finally, pile cross-sections and embedment depths were determined by the allowable displacement of the wall top, about 50 mm. Table 3 shows the embedment depth and pile diameter finally used in calculations.

2.4 *Random variables*

The uncertainty consisted of soil scatter, transformation error, model error, and others (Figure 3). The soil and rock had statistics for each random variable

Table 3. Embedment depth and wall stiffness finally used in each case. The values in the table represent d_e [m] (EI [MNm^2/m]).

d_0	N_r	$\Sigma\beta_i d_i$, a) 1.5 (short pile)	b) 2.0 (intermediate)	c) 3.0 (long pile)
1	50	3.48 (208)	4.06 (127)	5.64 (101)
	300	2.69 (169)	3.02 (90)	4.09 (72)
	1500	2.13 (114)	2.42 (71)	3.20 (59)
3	50	5.19 (753)	5.53 (321)	6.83 (165)
	300	4.48 (646)	4.76 (288)	5.82 (166)
	1500	4.08 (596)	4.25 (248)	5.04 (147)
5	50	5.83 (872)	6.06 (331)	7.47 (182)
	300	5.37 (646)	5.66 (294)	6.91 (197)
	1500	5.28 (646)	5.49 (282)	6.40 (186)

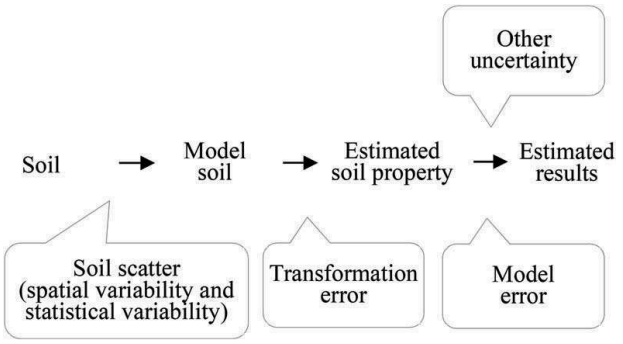

Figure 3. Types of uncertainty in ground property estimates.

with reference to previous works (Table 4). The load and the depth of the rock layer surface were also random variables. The subscripts s and r represent soil and rock, respectively. The transformation error from E_0 to k_H was omitted in this paper, though that COV was assumed 0.25 by Nanazawa et al. (2019). This was because the estimated total uncertainty was almost equal to that of the previous observations as shown later.

Table 4. Statistics of random variables.

	bias	COV	Distribution	Note	References
Soil scatter					
d_0	1.0	-	Normal	SD = 0.5m	Ohki et al. (2005)
N_s	1.0	0.3	Log-normal		Phoon et al. (1995)
γ_s	1.0	0.07	Log-normal	const.	Phoon et al. (1995)
N_r	1.0	0.3	Log-normal		
Transformation error from N-value					
E_{0s}	1.1	0.7	Log-normal	Eq. A2	PARI (2009), Nakatani et al. (2009)
$\tan\phi_s$	1.1	0.1	Log-normal	Eq. A1	Ching et al. (2016)
γ_r	1.0	0.07	Log-normal	Eq. A3	NEXCO RI (2016)
E_{0r}	1.5	1.2	Log-normal	Eq. A6	NEXCO RI (2016)
$\tan\phi_r$	1.2	0.2	Log-normal	Eq. A4	NEXCO RI (2016)
c_r	1.2	0.5	Log-normal	Eq. A5	NEXCO RI (2016)
Other uncertainty (Load and material)					
q_s	1.0	0.2	Normal		Phoon & Kulhawy (1999)
f_y	1.2	0.07	Log-normal		PARI (2009), Shiozaki et al. (2010)

The statistics of the log-normal variables are converted as;

$$\mu_{\ln X} = \ln \mu_X - \frac{1}{2}\sigma^2_{\ln X} \tag{2}$$

$$\sigma_{\ln X} = \sqrt{\ln\left[1 + \left(\frac{\sigma_X}{\mu_X}\right)^2\right]} \tag{3}$$

where the subscript $\ln X$ was a logarithm of a variable X.

Besides, although EN 1997-1 (2004) stated that the overdig should be considered as 10% of the wall height (limited to a maximum of 0.5 m) for Ultimate Limit State (ULS), it was not considered because the surface level was easy to be controlled in the situation of Figure 2a and Serviceability Limit State (SLS) was the primary target of the paper.

2.5 *Reliability analysis*

The elasto-plastic subgrade reaction method was difficult to formulate and obtain an exact analytical solution of the performance function at the design point. So, we calculated the difference of the performance function Z for $\pm$ $0.2\sigma_{Xi}$ and $0.4\sigma_{Xi}$ change in each random variable (Shiozaki et al. 2010) and conducted First-Order Reliability Method (FORM). The sensitivity factors are the normalized partial derivatives of the performance functions when there is no correlation between random variables (Figure 4):

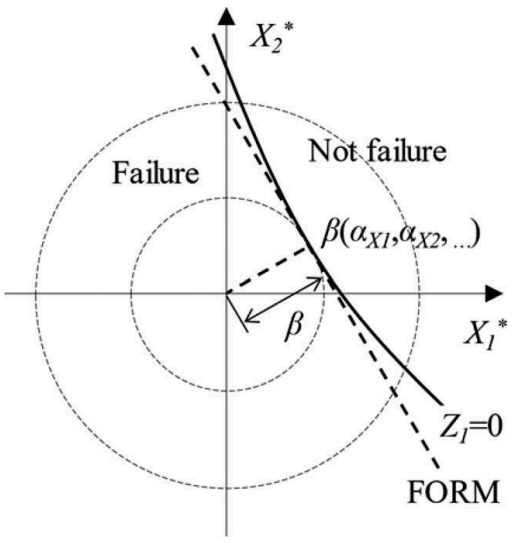

Figure 4. Illustration of FORM.

$$\alpha_{X_i} = \left(\frac{\partial Z}{\partial X_i}\bigg|_{X_f}\right) \cdot \frac{\sigma_{X_i}}{\sigma_Z} = \left(\frac{\partial Z}{\partial X_i^*}\bigg|_{X_f}\right) \cdot \frac{1}{\sigma_Z} \quad (4)$$

$$X_i^* = \left(X_i - \mu_{X_i}\right)/\sigma_{X_i} \quad (5)$$

where X_f represents the random variable X at the failure, which is defined as the state where the following performance functions Z are less than zero, respectively;

$$Z_{\delta_{top}} = \delta_a - \delta_{top}(X_i) \text{ (deformation failure)} \quad (6)$$

$$Z_M = M_y\left(f_y, S\right) - M_{\max}(X_i) \text{ (flexural failure)} \quad (7)$$

$$Z_{d_e} = d_e - d_{eq}(X_i) \text{ (rotational failure)} \quad (8)$$

The calculation points were around the deformation failure. Since they were not around the flexural failure, the calculated maximum bending stress was converted to the yield strength of the wall, *fy*, for comparison with other random variables.

3 ANALYSIS RESULT AND DISCUSSION

Figures 5, 6, and 7 show the contribution of uncertain sources and COVs to each performance function. The contribution factors were determined to be the squares of the sensitivity factors, and the COVs were the SDs divided by the means.

Firstly, COVs on the deformation failure decreased in the order of (a) rigid short piles, (b) intermediate piles, and (c) elastic long piles. As for rigid short piles (a), the distribution of the contribution factors changed as d_0 did. When the depth of the rock layer surface, d_0, was 1 m, the scatters of d_0 and the transformation error of E_{0r} were dominant, whereas when d_0 was 5 m, each parameter of the surface layer was dominant. An intermediate d_0 of 3 m shows a trend in between. These trends were also true for intermediate piles (b) and elastic long piles (c). Also, COVs were about 35% in the elastic long piles, which were generally consistent with the one reported by Honjo & Otake (2014) above (42%), and the assumption of this study could be reasonable.

Secondly, as for the flexural failure (Figure 6), the distributions of the contribution factors and COVs of (a), (b), and (c) did not differ significantly. Each parameter of the surface layer was dominant because the bending moment was mostly determined by the active earth pressure in the excavation area. The contribution of the scatter of d_0 was large when d_0 was 1 m. When d_0 was 5 m, the sensitivity factors of $\tan\phi_s$ in (c), was about 0.8, which is in good agreement with the report by Shiozaki et al. (2010) if the soil scatters of N_s and N_r are omitted.

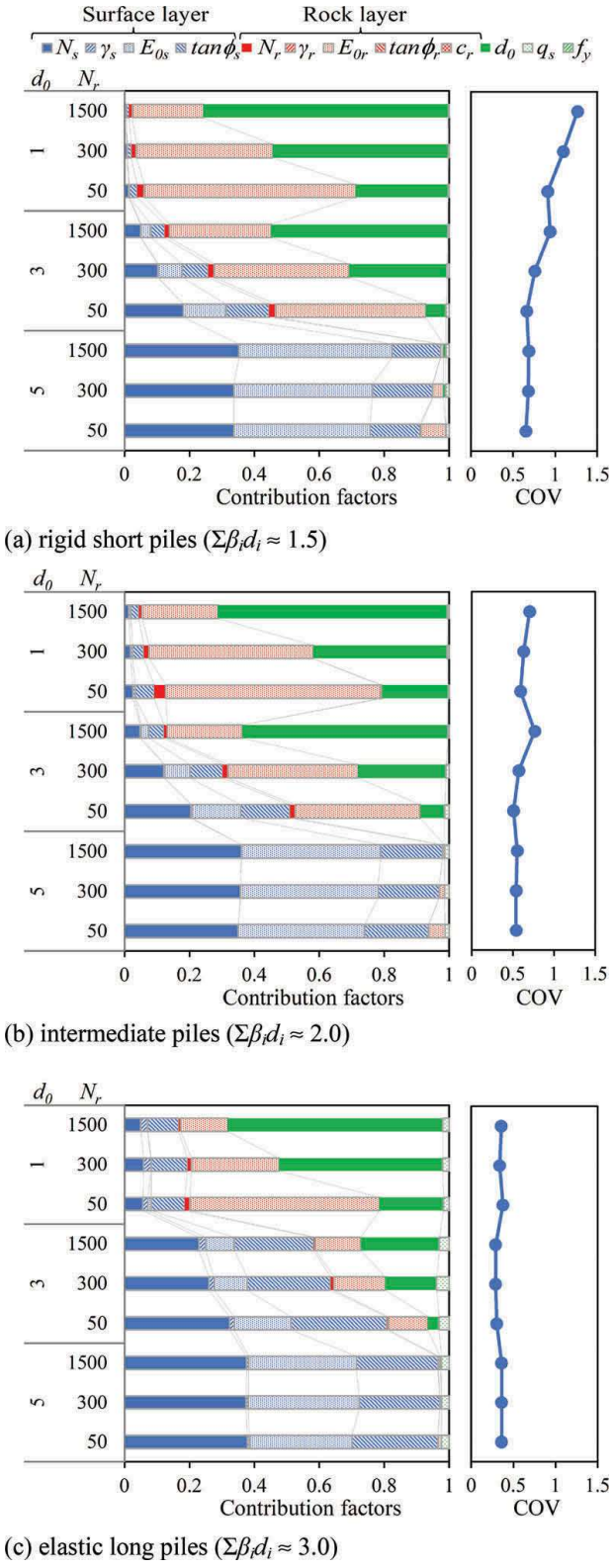

Figure 5. Contribution factors of uncertain sources and COVs of the performance function on the deformation failure.

Finally, in the case of rotational failure (Figure 7), since the performance function is independent of E_0, the contribution factors of E_0 are naturally zero. As in Figure 4, when d_0 was 1 m, the depth scatters of the rock layer surface and the transformation error of the strength of the rock layer (especially c_r) were

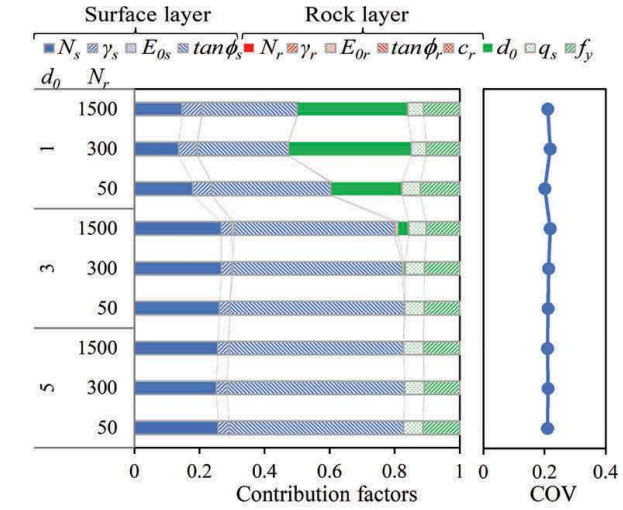

(a) rigid short piles ($\Sigma\beta_i d_i \approx 1.5$)

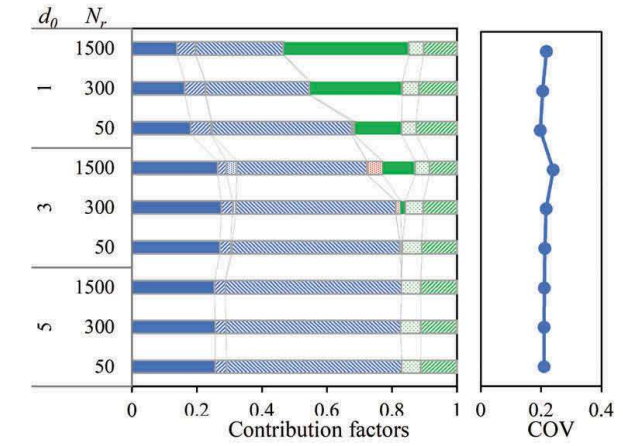

(b) intermediate piles ($\Sigma\beta_i d_i \approx 2.0$)

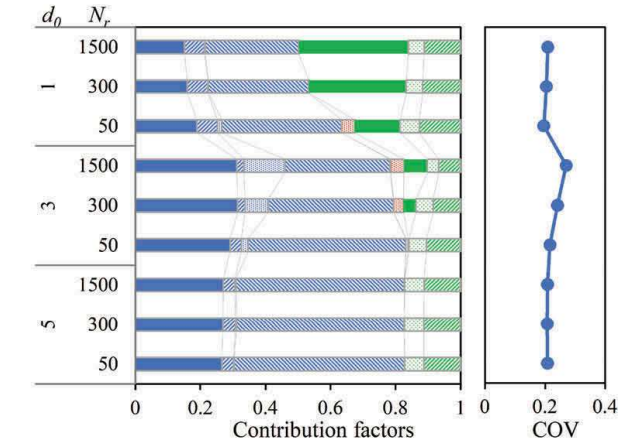

(c) elastic long piles ($\Sigma\beta_i d_i \approx 3.0$)

Figure 6. Contribution factors of uncertain sources and COVs of the performance function on the flexural failure.

dominant, whereas when d_0 was 5 m, each parameter of the surface layer is dominant.

COVs of the deformation failure depended on the stiffness factor (Figure 5), but those of the flexural failure did not (Figure 6). The distributions of the contribution factors depended on the depth and

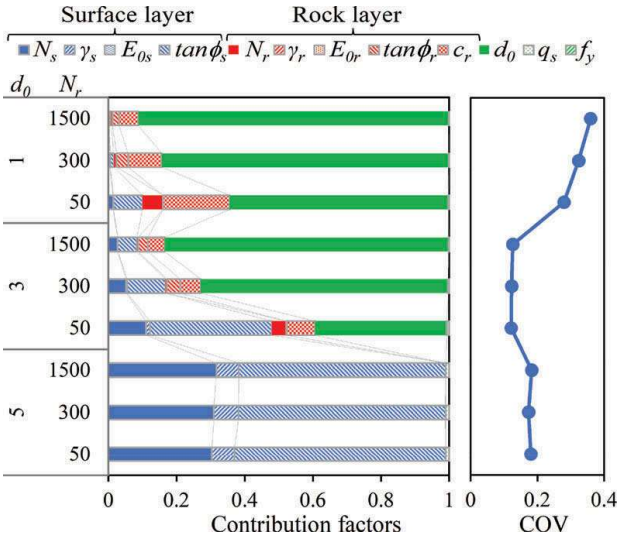

Figure 7. Contribution factors of uncertain sources and COVs of the performance function on the rotational failure.

N-value of the rock, but little on the stiffness factor. They result in that when the depth of the rock layer surface is shallow, the rigid short piles require larger safety margins of all variables especially the depth of the rock layer surface.

4 SUMMARY

In this paper, a reliability analysis was performed for cantilever steel pipe pile retaining walls embedded in the stiff ground, treating the uncertainty of the depth of the rock layer surface as variables. Since the sensitivity factors and COVs with sufficiently deep embedment were in good agreement with previous studies, the results of this study could be reasonable.

The following conclusions were drawn:

- The uncertainty of the depth of the rock layer surface had a significant contribution to each limit state in the order of rotational failure (ULS), deformation failure (SLS), and flexural failure (ULS).
- While COVs of the performance function on the deformation failure of the small stiffness factor were higher than those of the large stiffness factor, those on the flexural failure scarcely depended on the stiffness factor.
- The distributions of the contribution factors depended on the depth and N-value of the rock, but little on the stiffness factor.

When the contribution factor of the depth of the rock layer surface is large, it can be difficult to design cantilever walls rationally because we don't know its scatter in general. In this case, therefore, we believe that construction data that observe the

actual geotechnical situation directly improve the reliability of the structure.

Also, the quantitative sensitivity factors and contribution factors are useful for rational design and construction.

ACKNOWLEDGEMENTS

This study was conducted as part of IPA-TC1 (Application of cantilever type steel tubular pile wall embedded to the stiff ground).

REFERENCES

Bak Kong Low. 2017. EXCEL-Based Direct Reliability Analysis and Its Potential Role to Complement Eurocodes, *Joint TC205/TC304 Working Group on "Discussion of statistical/reliability methods for Eurocodes"*. – Final Report (Sep 2017)

Ching, J., Li, D. Q., & Phoon, K. K. 2016. Statistical characterization of multivariate geotechnical data. Chapter 4 in *Reliability of geotechnical structures in ISO2394*. Florida: CRC Press: 89–126.

EN 1997-1. 2004. *Eurocode 7: Geotechnical design. Part 1: General rules*. Belgium: European Committee for Standardization (CEN).

EN 1997-2. 2007. *Eurocode 7: Geotechnical design. Part 2: Ground investigation and testing*. Belgium: European Committee for Standardization (CEN): 24–29.

Gaba, A., Hardy, S., Doughty, L., Powrie, W. & Selemetas, D, 2017. *Guidance on embedded retaining wall design*. C760. London: CIRIA. https://www.ciria.org/ProductExcerpts/c760.aspx

Honjo, Y. & Otake, Y. 2014. Consideration on Major Uncertainty Sources in Geotechnical Design. *Second International Conference on Vulnerability and Risk Analysis and Management (ICVRAM) and the Sixth International Symposium on Uncertainty, Modeling, and Analysis (ISUMA), Liverpool, UK*: 2488–2497.

Ishihama, Y., Takemura, J. & V. Kunasegaram. 2019. Analytical evaluation of deformation behavior of cantilever type retaining wall using large diameter steel tubular piles into stiff ground, *The 4th International conference on geotechnics for sustainable development, GEOTEC Hanoi 2019*.

Japan Geotechnical Consultants Association (JGCA, or ZENCHIREN). 2017. *(Draft) Report of the Study Committee on "Investigating Method for Pile Foundations on Rock Layer"* (In Japanese) https://www.zenchiren.or.jp/geocenter/pdf/201701.pdf

Japan Road Association (JRA). 1999. *Road Earthwork, Guideline for the Construction of Temporary Structures*. Tokyo: JRA. (in Japanese)

Long, M. 2001. Database for retaining wall and ground movements due to deep excavations. *Journal of Geotechnical and Geoenvironmental Engineering*, 127(3): 203–224.

Michael Tomlinson & John Woodward, 2007. *Pile Design and Construction Practice*, Fifth Edition, Florida: CRC Press: p.330

Miyanohara Tomoko, Kurosawa Tatsuaki, Harata Noriyoshi, Kitamura Kazuhiro, Suzuki Naoki & Kajino Koji, 2018. Overview of the Self-standing and High Stiffness Tubular Pile Walls in Japan, *Proceedings of the First International Conference on Press-in Engineering 2018, Kochi*. IPA: Tokyo: 167–174.

Moormann, C. 2004. Analysis of wall and ground movements due to deep excavations in soft soil based on a new worldwide database. *Soils and foundations*, 44 (1): 87–98.

Nakatani S., Nanazawa, T., Shirato, M., Nishida, H., Kono, T. & Kimura, S., 2009. Research on Stability Verification Method of Highway Bridge Foundation in Performance Based System, *Public Works Research Institute Report* No.4136 (In Japanese)

Nanazawa, T., Kouno, T., Sakashita, G., & Oshiro, K. 2019. Development of partial factor design method on bearing capacity of pile foundations for Japanese Specifications for Highway Bridges. *Georisk: Assessment and Management of Risk for Engineered Systems and Geohazards*, 13(3): 166–175.

NEXCO RI. 2016. *Design Guide Vol. 2: Bridge Construction*. (In Japanese)

Nishioka Hidetoshi, Anzai Ayako & Koda Masayuki, 2010. Estimation of deformation modulus of ground and coefficient of subgrade reaction depending on ground investigation method. *RTRI report*, 24(7): 11–16 (in Japanese)

Ohki, H., Nagata, M., Saeki, E. & Kuwabara, H., 2005. Fluctuation on bearing strata levels of piles (part 2). *Proceedings of the 40th Technical Report of the Annual Meeting of the Japan Geotechnical Society, Japan*: 1549-1550 (In Japanese)

Osman, A. S., & Bolton, M. D. 2004. A new design method for retaining walls in clay. *Canadian geotechnical journal*, 41(3): 451–466.

Otake Yu, Nanazawa Toshiaki, Honjo Yusuke, Kono Tetsuya & Tanabe Akinori, 2017. Improvement of deformation modulus estimation considering soil investigation types and strain level, *Journal of Japan Society of Civil Engineers*, Ser. C (Geosphere Engineering), Volume 73 Issue 4: 396–411.

Phoon, K., & Kulhawy, F H. 1999. Evaluation of geotechnical property variability, *Canadian Geotechnical Journal*. 36(4): 625–639.

Phoon, K., Kulhawy, F H. & Grigoriu, M D. 1995. *Reliability-based design of foundations for transmission line structures*. Final report, Electric Power Research Inst., Palo Alto, EPRI-TR-105000

The Port and Airport Research Institute (PARI). 2009. *Technical standards and commentaries for port and harbour facilities in japan*. Part III FACILITIES, The Oversies Coastal Area Development Institute Japan, p.464 http://ocdi.or.jp/tec_st/tec_pdf/tech_364_551.pdf

Robert L. Parsons, Matthew C. Pierson, Isaac Willems, Jie Han & James J. Brennan, 2011. Lateral Resistance of Short Rock Sockets in Weak Rock: Case History. *Transportation Research Record Journal of the Transportation Research Board* 2212(-1): 34–41

Shiozaki, Y., Maeno, K., Otsushi, K., Kakimoto, R. & Ohtsuki, M. 2010. Partial Factors for Stress Verification of Self-Supporting Sheet Pile Quay Using Steel Pipe Sheet Pile. *Proceedings of the 65th Japan Society of Civil Engineers Annual Meeting, Japan*, II-094 (In Japanese)

Simpson, B. 2005. Eurocode 7 Workshop–Retaining wall examples 5-7. *In ISSMGE ETC23 workshop, Trinity College, Dublin*.

Sivakumar Babu, G. L. & Basha, B. M. 2008. Optimum design of cantilever retaining walls using target reliability approach. *International journal of geomechanics*, 8 (4): 240–252.

Suzuki N. & Kimura Y. 2021. Summary of case histories of retaining wall installed by rotary cutting press-in method. *Proceedings of the Second International Conference on Press-in Engineering 2021*, *Kochi* (under review)
Zhang, D. M., Phoon, K. K., Huang, H. W. & Hu, Q. F. 2015. Characterization of model uncertainty for cantilever deflections in undrained clay. *Journal of Geotechnical and Geoenvironmental Engineering*, 141(1).
Zhang, L. M. & Dasaka, S. M. 2010. Uncertainties in geologic profiles versus variability in pile founding depth. *Journal of Geotechnical and Geoenvironmental Engineering*, 136(11): 1475–1488.

APPENDIX 1

The transformation equations for the ground (sandy soil) from an N-value to ϕ and E_c are;

$$\phi = \sqrt{15N} + 20 \tag{A1}$$

$$E_c = 700N \tag{A2}$$

The transformation equations from a converted N-value of rock (sandstone) to γ, ϕ, c and E_c are as follows (NEXCO RI 2016), respectively;

$$\gamma = 1.7\ln(N) + 11.5 \tag{A3}$$

$$\phi = 5.10\ln(N)/2.3 + 29.3 \tag{A4}$$

$$\ln(c) = 0.327\ln(N) + 2.72 \tag{A5}$$

$$\ln(E_c) = 0.69\ln(N) + 7.9 \tag{A6}$$

The coefficient of the lateral subgrade reaction, k_H, is calculated from the deformation coefficient of the ground E_c, taking into account the size effect of the loading width B_H (= 10 m).

$$k_H = \left(\frac{4E_c}{0.3}\right)\left(\frac{B_H}{0.3}\right)^{-3/4} \tag{A7}$$

Nishioka et al. (2010) and Otake et al. (2017) are also helpful, which showed the relationship between the deformation coefficients for each geotechnical investigation method. It is also noted that the applicability of the subgrade reaction method for rock is not clear. The socket pile is a well-known structure embedded in bedrock, and the researches on them are informative though there are a few studies on the horizontal deformation (e.g. Robert et al. 2011).

Active and passive earth pressures, p_A and p_{Pu}, are calculated by the angle of shearing resistance, cohesion, and wall friction angle δ_f which is a constant of 15 degrees. Effective unit weight below the groundwater level is uniformly the unit weight minus 9 kN/m^3.

$$\begin{aligned} p_A &= \left[K_A\left(\sum \gamma z + q\right)\right]\cos\delta_f \\ K_A &= \frac{\cos^2\phi}{\cos\delta_f\left(1+\sqrt{\frac{\sin\left(\phi+\delta_f\right)\sin\phi}{\cos\delta_f}}\right)} \end{aligned} \tag{A8}$$

$$\begin{aligned} p_{Pu} &= \left[K_P\left(\sum \gamma z\right) + 2c\sqrt{K_P}\right]\cos\delta_f \\ K_P &= \frac{\cos^2\phi}{\cos\delta_f\left(1-\sqrt{\frac{\sin\left(\phi-\delta_f\right)\sin\phi}{\cos\delta_f}}\right)} \end{aligned} \tag{A9}$$

The differential equation of the lateral displacement, δ, is expressed using the depth z (upward direction is positive, and the depth at the excavation surface is zero);

$$\begin{aligned} EI\frac{d^4\delta}{dz^4} &= -pB \\ p &= \begin{cases} -p_A & (z>0) \\ \min(k_H\delta, p_{Pu}) & (z\le 0) \end{cases} \end{aligned} \tag{A10}$$

Where both ends of the wall are free, the equation can be solved under the four boundary conditions;

$$\begin{aligned} \left[EI\frac{d^3\delta}{dz^3}\right]_{z=H} &= 0, \left[EI\frac{d^3\delta}{dz^3}\right]_{z=-d_e} = 0 \\ \left[EI\frac{d^2\delta}{dz^2}\right]_{z=H} &= 0, \left[EI\frac{d^2\delta}{dz^2}\right]_{z=-d_e} = 0 \end{aligned} \tag{A11}$$

Young's modulus of elasticity of steel, E, is 2.0E +05 N/mm^2. The corrosion of the steel was not considered in this paper. The second moment, I, and the section modulus, S, of the steel pipe pile wall are;

$$I = \pi\left(D^4 - D_{in}^4\right)\pi/64 \tag{A12}$$

$$S = \pi\left(D^4 - D_{in}^4\right)/32D \tag{A13}$$

APPENDIX 2

Symbols and abbreviations are as follows.

B	m:	Unit wall width
B_H	m:	Equivalent Loading Width
D	m:	Outer pile diameter
D_{in}	m:	Inner pile diameter
d	m:	Installed pile depth
d_e	m:	Embedment depth
d_{eq}	m:	Critical embedment depth for extreme equilibrium
d_0	m:	Depth of the rock layer surface, or thickness of the surface layer
E	N/mm^2:	Young's modulus of elasticity of steel
E_c	N/mm^2:	Deformation coefficient of the ground (horizontal loading test in the borehole)
E_0	N/mm^2:	Deformation coefficient of the ground (flat-plate loading test)
f_y	N/mm^2:	Yield strength of steel
H	m:	Height of structures, that is excavation depth
I	m^4:	The second moment of area of the wall section
k_H	kN/m^3:	Coefficient of lateral subgrade reaction
K_A	-:	Active earth pressure coefficient
K_P	-:	Passive earth pressure coefficient
M_y	kNm/m:	Yield bending moment
M_{max}	kNm/m:	Maximum bending moment
N	-:	SPT N-value (blows per 300 mm penetration)
p_A	kN/m^3:	Active earth pressure

(*Continued*)

(Cont.)

p_{Pu}	kN/m^3:	Ultimate passive earth pressure
q_s	kN/m^3:	Any uniform surcharge at the ground surface
S	m^3:	Section modulus
t	mm:	Steel pile thickness
X_i	-:	Random variable
X^*	-:	Standardized value by the standard deviation
z	m:	Depth
Z	-:	Performance function
$Z_{\delta top}$	-:	Performance function on the deformation failure
Z_M	-:	Performance function on the flexural failure
Z_{de}	-:	Performance function on the rotational failure
α_i	-:	Sensitivity factor for i-th variable
β_i	m^{-1}:	Stiffness factor of i-th ground layer
γ	kN/m^3:	Effective unit weight of the ground
δ	m:	Displacement of wall
δ_a	m:	Allowable displacement
δ_f	degree:	Angle of friction between soil and wall
δ_{top}	m:	Displacement of wall top
μ	-:	Arithmetic mean
σ	-:	Bending stress
σ	-:	Standard deviation
ϕ	degree:	Angle of shearing resistance
COV	:	Coefficient of Variation
FORM	:	First Order Reliability Method
SD	:	Standard Deviation
SLS	:	Serviceability Limit State
ULS	:	Ultimate Limit State